Journal of Orthopaedic Translation (2018) 13, 13—24

Available online at www.sciencedirect.com

ScienceDirect

journal homepage: http://ees.elsevier.com/jot

ORIGINAL ARTICLE

Steroid-associated osteonecrosis animal model in rats

Li-Zhen Zheng [a], Jia-Li Wang [a], Ling Kong [a], Le Huang [a], Li Tian [a], Qian-Qian Pang [a], Xin-Luan Wang [c], Ling Qin [a,b,c,*]

[a] *Musculoskeletal Research Laboratory, Department of Orthopaedics & Traumatology, The Chinese University of Hong Kong, Hong Kong Special Administrative Region*
[b] *Innovative Orthopaedic Biomaterial and Drug Translational Research Laboratory, Li Ka Shing Institute of Health Sciences, The Chinese University of Hong Kong, Shatin, Hong Kong Special Administrative Region*
[c] *Translational Medicine R&D Center, Institute of Biomedical and Health Engineering, Shenzhen Institutes of Advanced Technology, Chinese Academy of Sciences, Shenzhen, PR China*

Received 4 October 2017; received in revised form 11 January 2018; accepted 12 January 2018
Available online 6 February 2018

KEYWORDS
Animal model;
Corticosteroid;
Osteonecrosis

Summary *Objective:* Established preclinical disease models are essential for not only studying aetiology and/or pathophysiology of the relevant diseases but more importantly also for testing prevention and/or treatment concept(s). The present study proposed and established a detailed induction and assessment protocol for a unique and cost-effective preclinical steroid-associated osteonecrosis (SAON) in rats with pulsed injections of lipopolysaccharide (LPS) and methylprednisolone (MPS).
Methods: Sixteen 24-week-old male Sprague—Dawley rats were used to induce SAON by one intravenous injection of LPS (0.2 mg/kg) and three intraperitoneal injections of MPS (100 mg/kg) with a time interval of 24 hour, and then, MPS (40 mg/kg) was intraperitoneally injected three times a week from week 2 until sacrifice. Additional 12 rats were used as normal controls. Two and six weeks after induction, animals were scanned by metabolic dual energy X-ray absorptiometry for evaluation of tissue composition; serum was collected for bone turnover markers, Microfil perfusion was performed for angiography, the liver was collected for histopathology and bilateral femora and bilateral tibiae were collected for histological examination.
Results: Three rats died after LPS injection, i.e., with 15.8% (3/19) mortality. Histological evaluation showed 100% incidence of SAON at week 2. Dual energy X-ray absorptiometry showed significantly higher fat percent and lower lean mass in SAON group at week 6. Micro-computed tomography (Micro-CT) showed significant bone degradation at proximal tibia 6 weeks after SAON induction. Angiography illustrated significantly less blood vessels in the

* Corresponding author. Rm74026, 5/F, Clinical Science Building, Prince of Wales Hospital, Shatin, Hong Kong Special Administrative Region.
E-mail address: lingqin@cuhk.edu.hk (L. Qin).

https://doi.org/10.1016/j.jot.2018.01.003

proximal tibia and significantly more leakage particles in the distal tibia 2 weeks after SAON induction. Serum amino-terminal propeptide of type I collagen and osteocalcin were significantly lower at both 2 and 6 weeks after SAON induction, and serum carboxy-terminal telopeptide was significantly lower at 6 weeks after SAON induction. Histomorphometry revealed significantly lower osteoblast surface and higher marrow fat fraction and oedema area in SAON group. Hepatic oedema appeared 2 weeks after SAON induction, and lipid accumulation appeared in the liver of SAON rats 6 weeks after SAON induction.

Conclusion: The present study successfully induced SAON in rats with pulsed injection of LPS and MPS, which was well simulating the clinical feature and pathology. Apart from available large animal models, such as bipedal emus or quadrupedal rabbits, our current SAON small model in rats could be a cost-effective preclinical experimental model to study body metabolism, molecular mechanism of SAON and potential drugs developed for prevention or treatment of SAON.

The translational potential of this article: The present study successfully induced SAON in a small animal model in rats with pulsed injection of LPS and MPS. The evaluation protocols with typical histopathologic ON features and advanced evaluation approaches to identify the metabolic disorders of SAON could be used in future rat SAON studies. The SAON rat model is a suitable and cost-effective animal model to study molecular mechanism of SAON and potential drugs developed for prevention and treatment of SAON.

Introduction

Steroid-associated osteonecrosis (SAON) is a multifactorial bone metabolic disease occurred after long term or/and large dose of corticosteroid therapy attributed to its anti-inflammatory and immunomodulatory effects [1]. The pathophysiology underlying the development of SAON includes fat embolism, vascular thrombosis, osteocyte and osteoblast apoptosis and oxidative stress [2]. However, the underlining pathogenesis of SAON is desirable to be studied by using suitable animal model(s).

Successfully established SAON rabbit model has been reported, with a clinically orientated induction protocol composed of a single injection of low dose of lipopolysaccharide (LPS) and subsequently three injections of high dose of methylprednisolone (MPS) with high incidence of SAON and low incidence of mortality [3]. For studying molecular mechanism of such metabolic diseases and drug prevention or treatment effects, rats are more suitable as they have been regarded as cost-effective animal models. So far, there are several reports on SAON rat models, but the protocols to induce SAON are different [4–8]. LPS could increase the incidence of SAON in animal models [5]. The dose of LPS in the published protocols ranged from 10 μg/kg to 2 mg/kg to induce SAON in rats [8,9]. The dose of LPS used in the rabbit SAON model is 10 μg/kg [3], but because rats are resistant to LPS, whereas rabbits are sensitive to LPS [10], we should use higher dose of LPS to induce SAON in the rat model than that used in the rabbit model. A preliminary study showed that the injection of 1 mg/kg LPS could induce 50% mortality in 24-week-old male Sprague–Dawley rats [11]; therefore, in this study, we tested the dose of LPS at 0.2 mg/kg that might reduce the mortality. In a clinical situation, high dose of pulsed MPS intravascularly (30 mg/kg) is prescribed to severe inflammation patients to rescue their life [12]. As smaller animals have higher metabolic rates and require larger drug dose per body weight, we calculated dose conversion between rat and human being by multiple clinical higher dose based on a published work [13]. To mimic the clinical situation, we tested the experimental protocol to induce SAON in rats with a single injection of high dose of LPS (0.2 mg/kg) and followed subsequently by pulsed injections of high dose of MPS (100 mg/kg). As SAON may get repaired spontaneously in quadrupedal animals, it is essential to inhibit repairing of the osteonecrosis. Accordingly, we continually gave rats sustained low dose of MPS (40 mg/kg) from week 2 to week 6 before harvesting specimens for analysis. For determining the age of rats used in this study, unlike humans and rabbits, it is problematic to determine adulthood using skeletal maturity because there is no closed growth plate in long bones in rats. For Sprague–Dawley rats, the skeletal growth tapers off at approximately 7–8 months [14]; therefore, we used 24-week-old young adult rats for the present study as this was the age where rat femoral head matured [15].

We hypothesised that a combination of LPS and MPS injections described above might also be able to induce SAON in rats. Accordingly, we evaluated the induction protocol at two time points, i.e., 2 and 6 weeks after SAON induction. We used different evaluation approaches to examine the effects of LPS and MPS in inducing metabolic disorders on the bone and other affected tissues. Histological examination was used to identify osteonecrotic lesions in bilateral femora and bilateral tibiae. Metabolic dual energy X-ray absorptiometry (DXA) was used for evaluation of tissue composition, i.e., fat and lean composition, to evaluate the effects of corticosteroid on fat and muscle metabolism. Serum bone turnover markers were quantified for determining the dynamics of bone turnover in this corticosteroid-

affected metabolic bone disorder. Angiography in bone marrow was imaged and evaluated by Microfil perfusion and micro-CT to define the vessel changes. Liver histopathology was used to identify the metabolic disorders in the liver. Establishing and validating preclinical disease models are essential for understanding the pathophysiology of the disease and testing prevention and/or treatment concept(s) with targeted mechanisms.

Materials and methods

Ethics statement

The Animal Experimental Ethics Committee of the principal investigator's institution reviewed and approved the experimental protocols (Ref. No. 15-150-MIS). Both the Guide for the Care and Use of Laboratory Animal (1996) [16] and the ARRIVE (Animals in Research: Reporting *In Vivo* Experiments) guidelines [17] were followed.

Experimental animals and study design

Twenty-eight 24-week-old male Sprague–Dawley rats (body weight 500∼600 g) were used in this study. All animals were housed in a temperature-controlled room (25°C) under a 12/12-hour reversed day/night cycle and received food and water *ad libitum*.

Animals were divided and allocated to normal control group (n = 12) and SAON group (n = 16). The SAON induction procedures for the SAON group are shown in Fig. 1. At day 1, under anaesthesia [90 mg/kg (ketamine) and 10 mg/kg (xylazine) intraperitoneally], each rat was intravenously injected with lipopolysaccharide (LPS, 0.2 mg/kg, Escherichia coli O111:B4; Sigma–Aldrich, St. Louis, MO, USA) via tail vein steadily and slowly. The LPS injection time was controlled for 30 minutes. At day 2, 3 and 4, three intraperitoneal injections of high-dose methylprednisolone (MPS, 100 mg/kg body weight, Pfizer Manufacturing Belgium NV, Puurs, Belgium) were given, and then, low-dose MPS (40 mg/kg, i.p.) were given three times a week at week 2–6. The rats were euthanised by intravenous injection of overdose of pentobarbital at the end of week 2 and week 6. Bilateral femora and tibiae, liver and blood of each rat were collected for further analysis (Fig. 1).

Dual energy X-ray absorptiometry

Rats were scanned at baseline, week 2 and week 6 (n = 6 for each time point). Scans were analysed using UltraFocus Digital Radiography System (Faxitron Bioptics, LLC, USA) at lower limbs for tissue composition (lean mass and fat percent). The region of interest (ROI) was defined as an oval shape with a size of 0.8–1.0 cm^2 adjacent to the lateral tibia but not including any bone tissue (Fig. 4B).

Micro-CT–based trabecular architecture

To determine the trabecular architecture, the tibiae from week 6 of each group were fixed in buffered formalin for one week and then were scanned using an animal micro-CT system (μCT-40; Scanco Medical, Brüttisellen, Switzerland). The trabecular bone with thickness of 2 mm and 2 mm from the growth plate was used as the ROI for analysis. The spatial resolution was set at 15 μm. A threshold of 220 HU and a low-pass Gaussian filter (Sigma = 0.8, Support = 1) were used to define mineralised tissue from the background signal [18]. The bone mineral density (BMD), bone tissue volume fraction (BV/TV), structure model index (SMI), connective density (Conn. D.), trabecular number (Tb. N), trabecular thickness (Tb. Th) and trabecular separation (Tb. Sp) were quantified [19].

Micro-CT–based angiography

Perfusion and decalcification: Under general and deep anaesthesia with intravenous administration of 2.5% sodium pentobarbital, the abdomen cavity of the rats were opened for perfusion with a confected radiopaque silicone rubber (Microfil MV-122; Flow Tech, Inc., Carver, MA, USA) via the abdominal aorta using our previously established protocol (n = 4/group) [3,20,21]. The animals were then sacrificed and stored at 4°C for full polymerisation of the *in vivo* injected Microfil. The excised tibiae were decalcified by 10% EDTA (pH 7.4). The decalcification process was assessed radiographically to confirm complete decalcification, i.e., without radiographic opacity.

Microangiography: The decalcified tibiae were scanned using a μCT-40 imaging system with the same protocol as used for imaging the trabecular bone. For proximal tibia, a cylinder with 3 mm thickness, 3 mm diameter and 2 mm

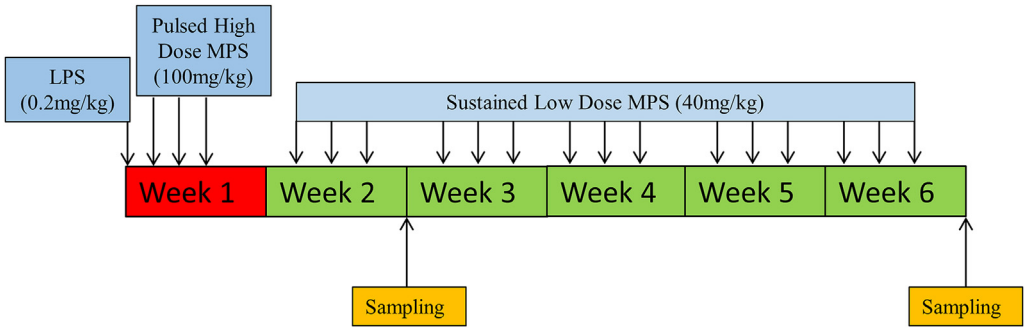

Figure 1 Steroid-associated osteonecrosis (SAON) induction protocol.
LPS = lipopolysaccharide; MPS = methylprednisolone.

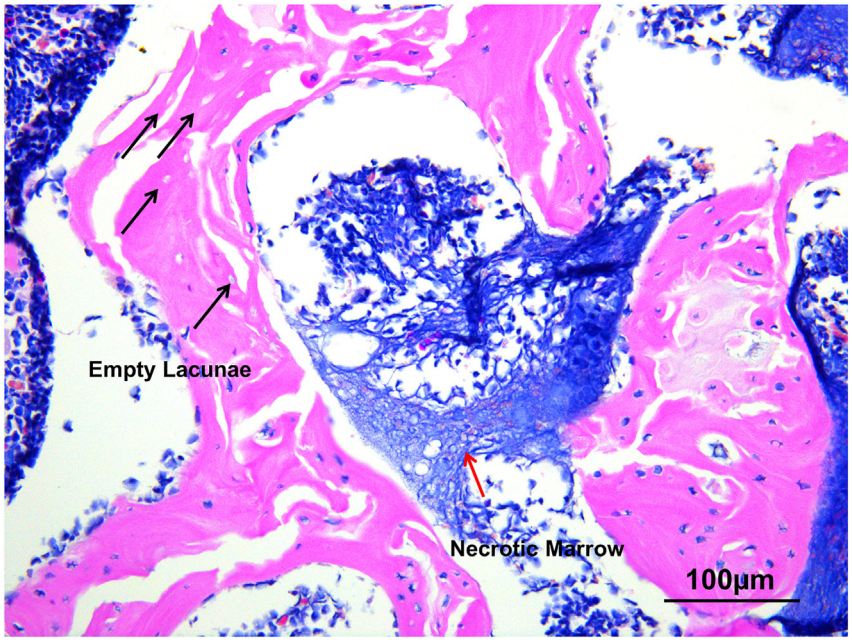

Figure 2 SAON identification by histology. A typical ON+ region in proximal femur in the SAON group 2 weeks after SAON induction. ON+ region showed empty lacunae (black arrow) in osteocytes and necrotic bone marrow (red arrow), surrounding with ON- region with normal osteocyte and normal marrow.
ON+ = osteonecrosis-positive; ON- = osteonecrosis-negative; SAON = steroid-associated osteonecrosis.

from the growth plate was used as the ROI; and for distal tibia, the 3-mm—thick whole bone marrow region from the distal end was used as the ROI. To segregate the infused radiopaque substance from the background, a low-pass Gaussian filter (Sigma = 1.2, Support = 2, threshold = 120 HU) was used [22]. Three-dimensional angiographic architecture images were reconstructed. Subtotal volume of the perfused Microfil in ROIs was calculated by summing volumes of the perfused Microfil in three groups: Small-sized (<100 μm), medium (100—200 μm) and large-sized (>200 μm) Microfil. A histogram was generated to display the thickness of the perfused Microfil [3,22].

Serum markers measurement

Before euthanasia, blood was collected via cardiac puncture for serum isolation that was then stored at −80°C before the biomarkers assay. Bone formation marker, including amino-terminal propeptide of type I collagen (PINP) and osteocalcin (OC), and bone resorption marker, carboxy-terminal telopeptide (CTX), were assayed using enzyme-linked immunosorbent assay (ELISA) kits (IDS Ltd., Boldon, UK) [23].

Histological and histomorphometrical analysis

The proximal and distal femora and proximal and distal tibiae were decalcified by 10% EDTA (pH 7.4), embedded in paraffin and cut into 5-μm—thick sections along the coronal plane. The livers were fixed in buffered formalin, embedded in paraffin and cut into 5-μm—thick sections. Sections were stained with haematoxylin and eosin (H&E), and tartrate-resistant acid phosphatase staining (Sigma Diagnostics, Missouri, USA) was performed for osteoclast accounts. The Microfil-perfused tibiae were paraffin sectioned, and the vascular endothelial growth factor (VEGF) expression in bone marrow was tested by immunohistochemistry with antibody VEGF (sc-7269) (SC; Santa Cruz, CA, USA).

Digital histological images were captured with a microscopic imaging system (Leica DM5500; Leica Microsystems, Wetzlar, Germany). The presence of osteonecrosis (ON) was examined with the established criteria, i.e., diffused presence of empty lacunae or pyknotic nuclei of osteocytes in trabecular bone accompanied by surrounding necrotic bone marrow [24]. The rat with at least one ON lesion in the proximal femur, distal femur, proximal tibia or distal tibia was considered as ON + rat, whereas that with no ON lesion was considered as ON− rat. Histomorphometric analysis was carried out on the metaphysis of the proximal tibia in a 2-mm—wide area 2 mm below the growth plate, and 3-mm—wide area of bone marrow from the end of the distal tibia using OsteoMeasure Histomorphometry System (Osteometrics Inc, Atlanta, GA, USA) and analysed according to a standard histomorphometry protocol [25]. The osteoblast surface (Ob. S/BS), osteoclast number (N.Oc/BS) and marrow fat fraction were determined on the red marrow region in the proximal tibia, and marrow oedema fraction was determined on the yellow marrow region in the distal tibia.

Statistical analysis

The incidence of ON was defined as the number of ON + rats divided by the total number of rats in each group and was analysed with Fisher's exact test. All numeric data

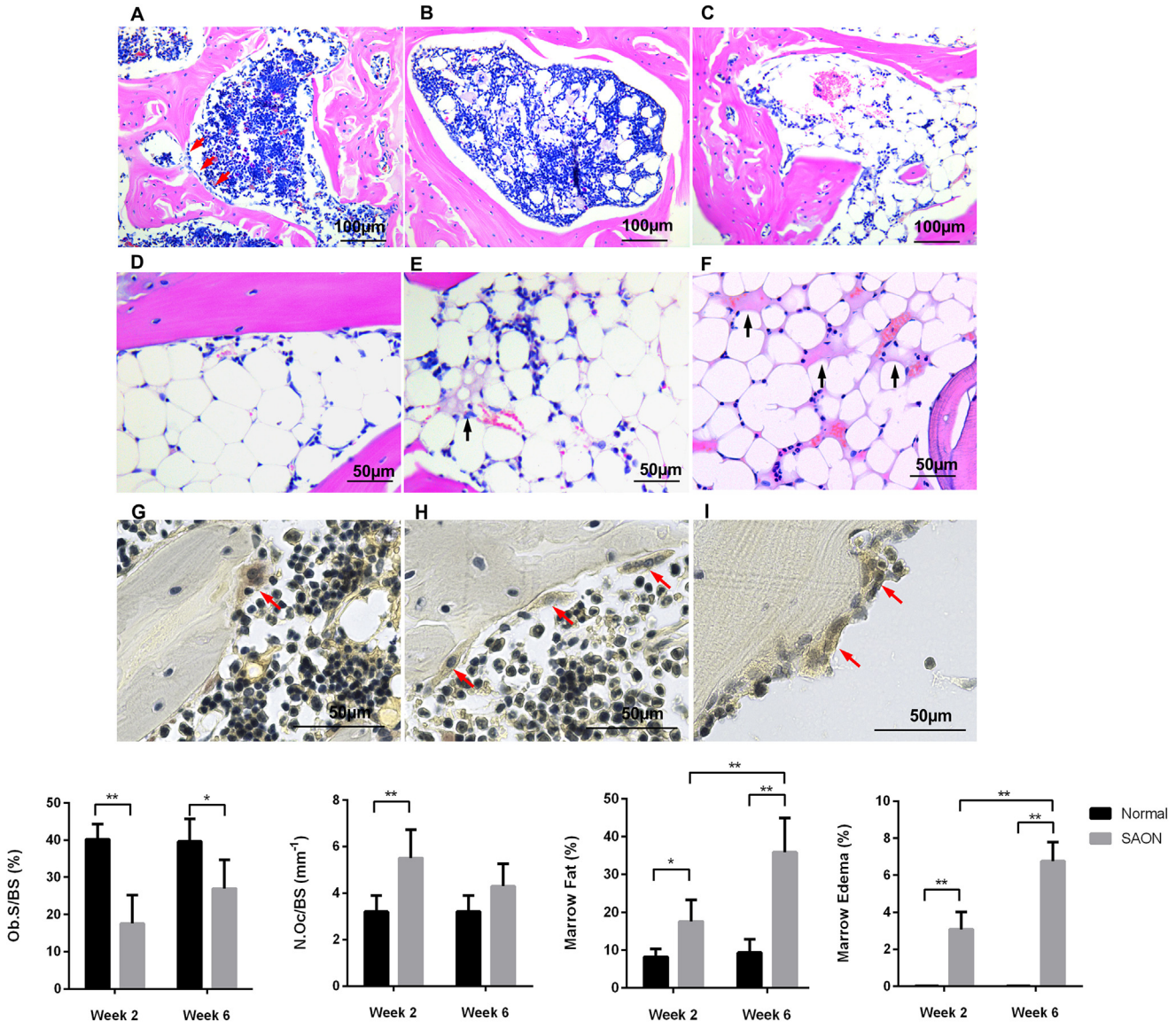

Figure 3 (A) Typical trabeculae and red marrow in the proximal tibia in the normal control group; (B) the proximal tibia in the SAON group 2 weeks after SAON induction; (C) the proximal tibia in the SAON group 6 weeks after SAON induction; (D) dense adipocytes in yellow marrow in the distal tibia of normal control rats; (E) 2 weeks after SAON induction, oedema (black arrow) was shown in yellow marrow in the distal tibia; (F) 6 weeks after SAON induction, more oedema (black arrow) appeared in yellow marrow in the distal tibia; (G) TRAP staining showed osteoclast (red arrow) in normal control group; (H) TRAP staining showed osteoclast (red arrow) 2 weeks after SAON induction the proximal tibia; (I) TRAP staining showed osteoclast (red arrow) 6 weeks after SAON induction in the proximal tibia. Histomorphometry results showed significantly lower osteoblast surface (Ob. S/BS) in the SAON group in both week 2 and week 6 in the proximal tibia (refer to A, B and C), significantly higher osteoclast number (N.Oc/BS) in the SAON group in week 2 in the proximal tibia (refer to G, H and I) and significantly higher marrow fat fraction in the proximal tibia of the SAON group in both week 2 and week 6 (refer to A, B and C). The marrow fat faction was significantly higher in week 6 than that in week 2 in the SAON group in the proximal tibia (refer to B and C). Typical marrow without oedema in the normal control group, obvious oedema in the SAON group in both week 2 and week 6 and significantly higher oedema in SAON group in week 6 than that in week 2 in the distal tibia were observed (refer to D, E and F). (*: $p < 0.05$, **: $p < 0.01$, n = 6).
ON+ = osteonecrosis-positive; ON- = osteonecrosis-negative; SAON = steroid-associated osteonecrosis; TRAP = tartrate-resistant acid phosphatase.

were expressed as mean ± SD with unpaired two-tailed *t* test or two-way analysis of variance (data with different time point) followed by Bonferroni posttest to assess statistical significance between groups. Statistical analysis was performed using SPSS 17.0 software (Chicago, IL, USA). A p value < 0.05 was considered statistically significant.

Results

Mortality rate and incidence of SAON

Rats of the SAON group were lethargic and anorexic at the first week after administration of LPS. Two rats died at day

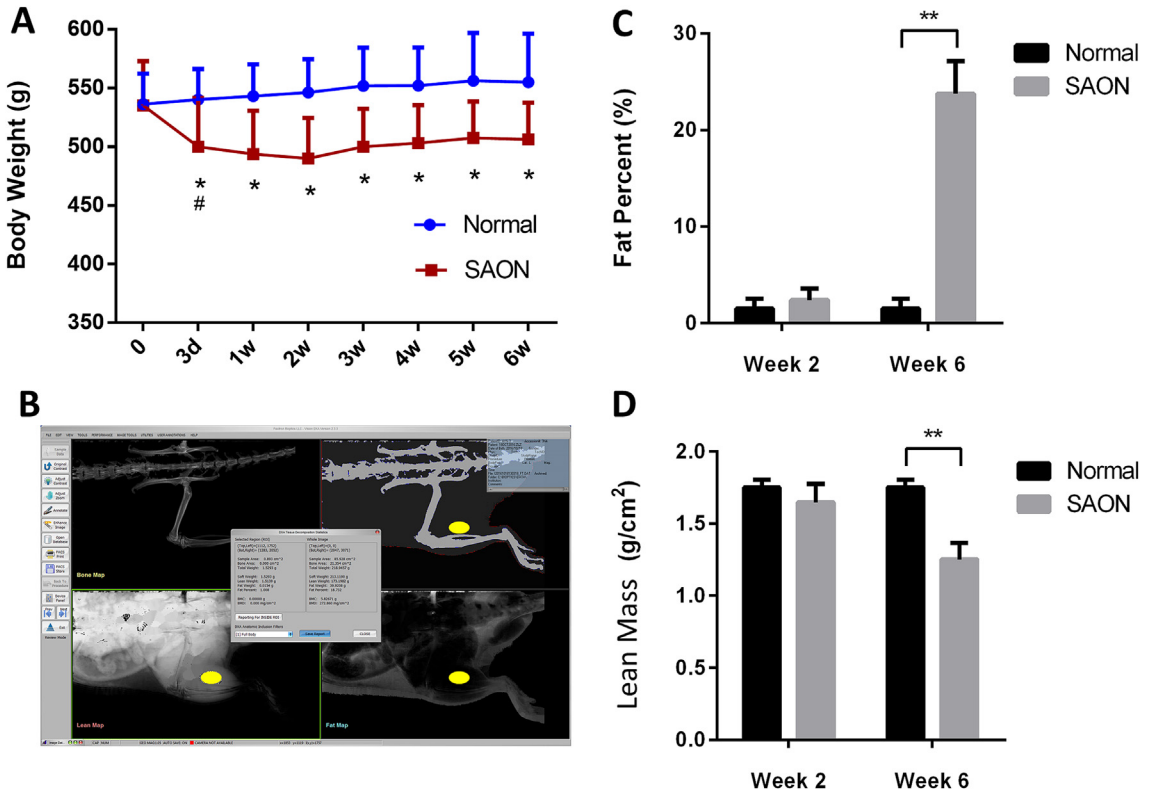

Figure 4 (A) The body weight of the SAON group rats were significantly lower 3 days after SAON induction (#: $p < 0.05$ compared between time points) and after that lower than that of the normal group rats (*: $p < 0.05$ compared between groups). (B) Animal dual energy X-ray absorptiometry (DXA) analysis on an oval-shaped region with a size of 0.8—1.0 cm^2 adjacent to the lateral tibia but not including any bone tissue (yellow oval); (C) results showed that there was no significant difference between the SAON group and normal group for fat percent at week 2, whereas at week 6, the fat percent of the SAON group was significantly higher; (D) results showed that there was no significant difference between the SAON group and normal group for lean mass at week 2, whereas at week 6, the lean mass of the SAON group was significantly lower (**: $p < 0.01$, n = 6).
SAON = steroid-associated osteonecrosis.

2, and one died at day 3 after LPS injection; three additional rats were supplemented for replacement. The total mortality rate was 15.8% (3/19). The acute sicknesses were recovered at the second week. We defined the osteonecrosis-positive (ON+) and osteonecrosis-negative (ON−) region by histological analysis on H&E-stained sections with the established criteria: the ON + region showed diffused presence of empty lacunae or pyknotic nuclei of osteocytes in trabecular bone accompanied by surrounding necrotic bone marrow, whereas ON− region showed normal osteocyte with surrounding normal bone marrow [24]. At week 2, all the rats developed osteonecrosis based on histological evaluation with 100% incidence of SAON (8/8). Empty lacunae of osteocytes were found in the trabeculae. Oedema and fibrous marrow appeared in necrotic bone marrow. At week 6, six rats showed oedema and fibrous marrow and empty lacunae of osteocytes with 75% incidence of SAON (6/8). The proximal femur was the site of highest instance of ON 2 weeks after induction. At week 6, the instances of ON in the proximal femur, distal femur and proximal tibia were significantly decreased when compared with those at week 2, whereas the instance of ON in the distal tibia did not change statistically (Fig. 2 and Table 1).

Body weight and tissue composition at the lower limb

The body weight of SAON group rats were significantly lower 3 days after SAON induction ($p < 0.05$ compared between time points) and after which it was lower than that of the normal group rats ($p < 0.05$ compared between

Table 1 Prevalence of ON lesions.

Group		Number of ON cases (Number of bones examined)			
		Proximal femur	Distal femur	Proximal tibia	Distal tibia
Week 2	Normal	0 (12)	0 (12)	0 (12)	0 (12)
	SAON	14 (16)	9 (16)	8 (16)	4 (16)
Week 6	Normal	0 (12)	0 (12)	0 (12)	0 (12)
	SAON	6 (16)[a]	1 (16)[a]	1 (16)[a]	6 (16)

[a]: $p < 0.05$, compared between week 2 and week 6. Bilateral skeletal sites were examined.
ON = osteonecrosis; SAON = steroid-associated osteonecrosis.

groups). DXA analysis showed that there was no significant difference between the SAON group and normal group for both percentage fat and lean mass at week 2; whereas at week 6, the percentage fat of SAON group was significantly higher, and the lean mass of SAON group was significantly lower ($p < 0.01$, n = 6) (Fig. 4).

Micro-CT—based trabecular architecture

Trabecular architecture of the proximal tibia was analysed using micro-CT. Six weeks after SAON induction, the BMD, BV/TV, Conn. D. and Tb. N of the SAON group were all significantly lower than those in the normal control group ($p < 0.05$, n = 6); the Tb. Sp of the SAON group was significantly higher than that in the normal group ($p < 0.05$, n = 6); whereas there was no significant difference in the SMI and the Tb. Th between the two groups (Fig. 5).

Micro-CT—based angiography

Vessel architecture in the proximal tibia and distal tibia in the normal and SAON group was analysed by Microfil perfusion and micro-CT. Histogram showed that in the proximal tibia, the medium (100—200 μm) and large-sized (>200 μm) blood vessels in the SAON group were significantly less than those in the normal group; in the distal tibia, the small-sized

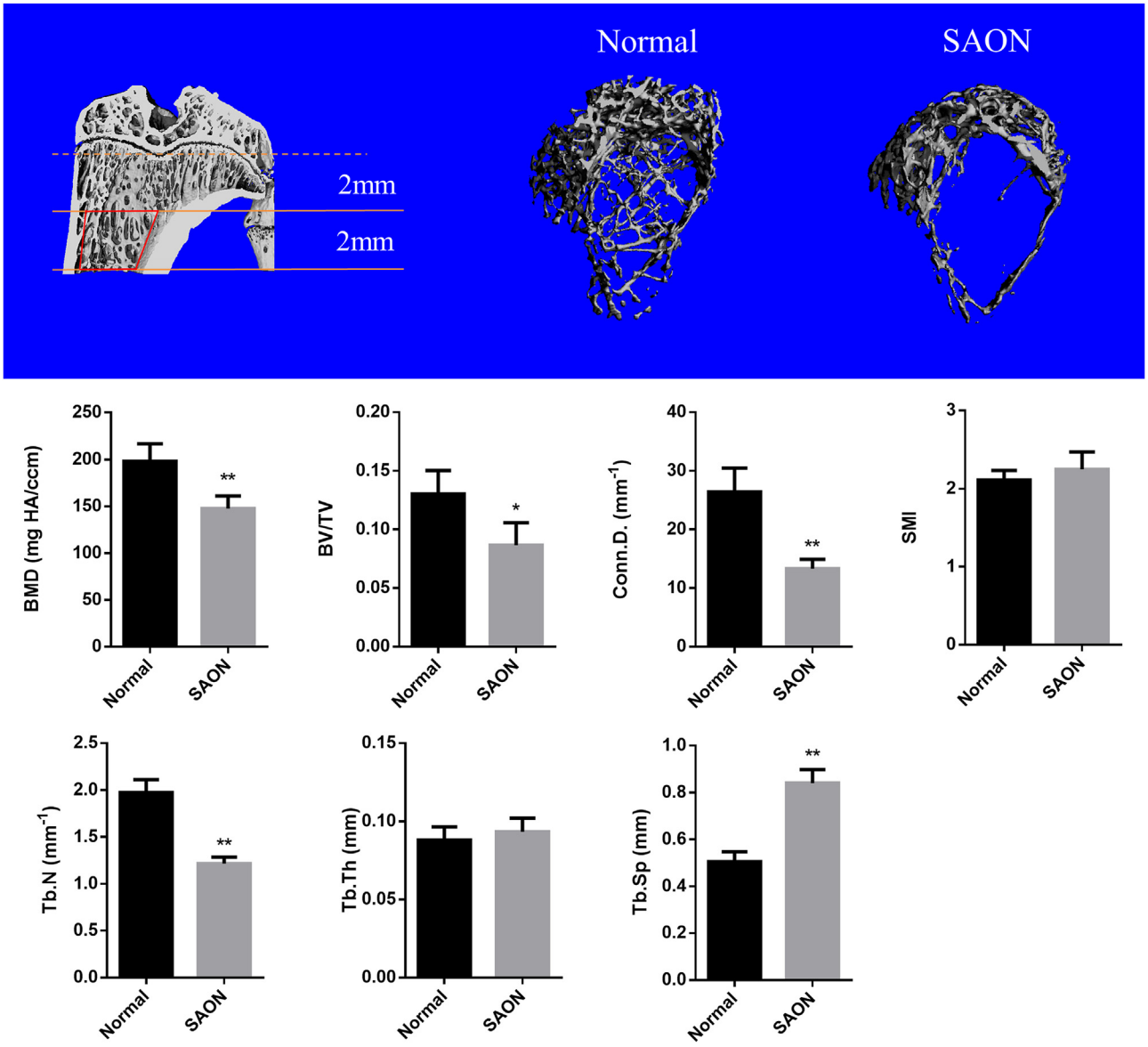

Figure 5 Micro-CT—based trabecular architecture. Representative micro-CT 3-D images and quantitative analysis of the trabecular bone of the proximal tibia (red box showed the ROI). 6 weeks after SAON induction, the bone mineral density (BMD), bone tissue volume fraction (BV/TV), connective density (Conn. D.) and trabecular number (Tb. N) of the SAON group were all significantly lower than those in the normal control group; the trabecular separation (Tb. Sp) of the SAON group was significantly higher than that in the normal group; while there was no significant difference for the structure model index (SMI) and the trabecular thickness (Tb. Th) between the two groups. (*: $p < 0.05$, **: $p < 0.01$, n = 6).
SAON = steroid-associated osteonecrosis.

leakage particles (<100 μm) in the SAON group were significantly more than those in the normal group ($p < 0.05$, n = 4). Histologic sections showed that the small-sized leakage particles were in the bone marrow outside the blood vessels (Fig. 6C1). VEGF expression was higher in the SAON group in both proximal and distal tibia (Fig. 6).

Serum markers

For bone turnover markers, serum PINP and OC in the SAON group were significantly lower at both week 2 and week 6 than those in the normal group; serum CTX in the SAON group was significantly lower at week 6 than that in the normal group at the same time point and that at week 2 in the SAON group. ($p < 0.05$, n = 6) (Fig. 7).

Histomorphometry

Histomorphometry results showed significantly lower Ob.S/BS in the SAON group in both week 2 and week 6 and significantly higher osteoclast number (N.Oc/BS) in the SAON group in week 2. Significantly higher marrow fat fraction was found in the SAON group in both week 2 and week 6. The marrow fat faction was significantly higher in week 6 than that in week 2 in the SAON group. No marrow oedema in the normal control group, significantly higher oedema area in the SAON group in both week 2 and week 6, and significantly higher oedema area in the SAON group in week 6 than that in week 2 ($p < 0.05$, n = 6) (Fig. 3) were observed.

Liver histopathologic examination

H&E staining showed regular hepatic cells in normal rats. Hepatic oedema appeared 2 weeks after SAON induction; cell division suggested hepatic injury and repair progress. The acute hepatic injury was repaired 6 weeks after SAON induction, while lipid accumulation appeared in SAON rats 6 weeks after SAON induction. Different from the oedema in the H&E staining sections that showed cavity inside the

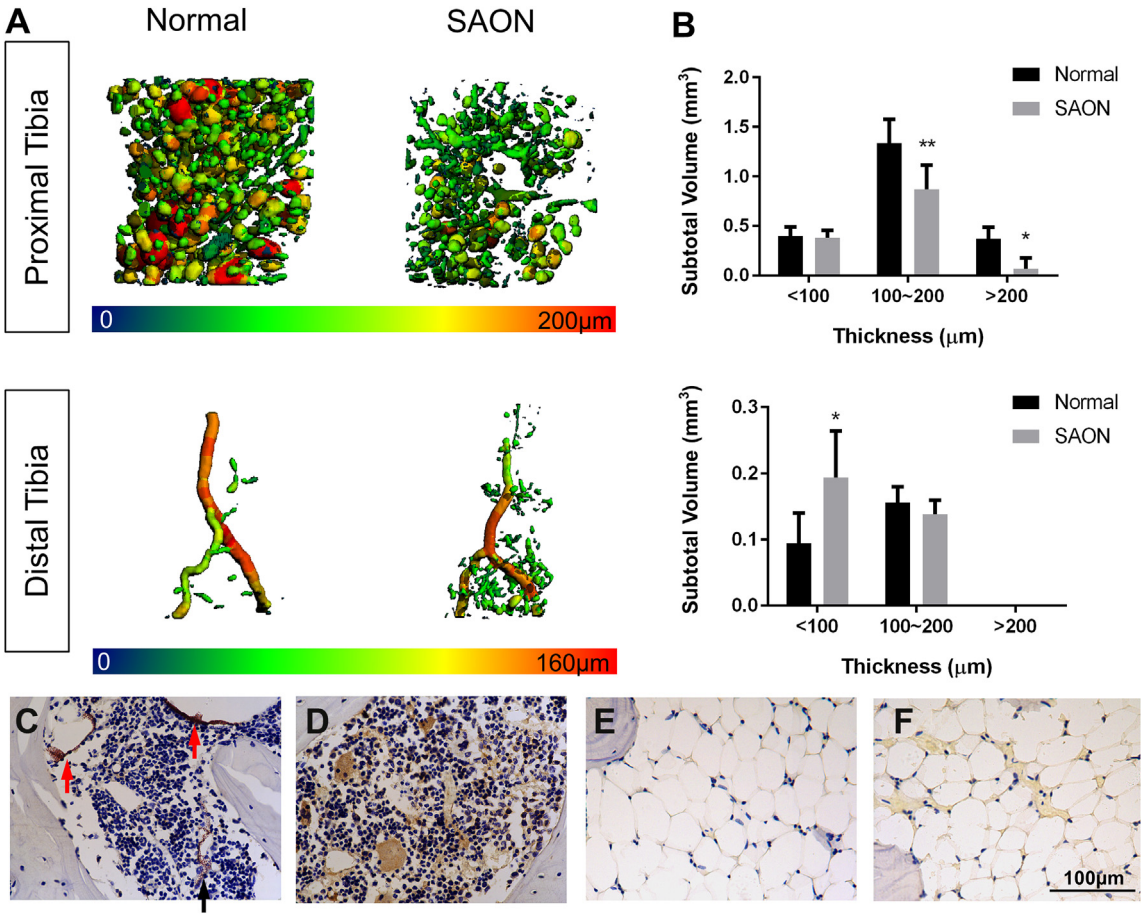

Figure 6 (A) Representative 3-D images of micro-CT based vessel architecture in the proximal tibia and distal tibia in the normal and SAON group; (B) histogram showed that in the proximal tibia, the medium (100—200 μm) and large-sized (>200 μm) blood vessels in the SAON group were significantly less than those in the normal group and in the distal tibia, the small-sized leakage particles (<100 μm) in the SAON group were significantly more than those in the normal group (*: $p < 0.05$, **: $p < 0.01$, n = 4); (C) proximal tibia from the normal group (red arrow: Microfil in blood vessel; black arrow: leakaged Microfil particles); (D) proximal tibia from the SAON group; (E) distal tibia from the normal group; (F) distal tibia from the SAON group. Representative immunohistochemistry staining showed higher VEGF expression in the SAON group in both proximal and distal tibia.
SAON = steroid-associated osteonecrosis.

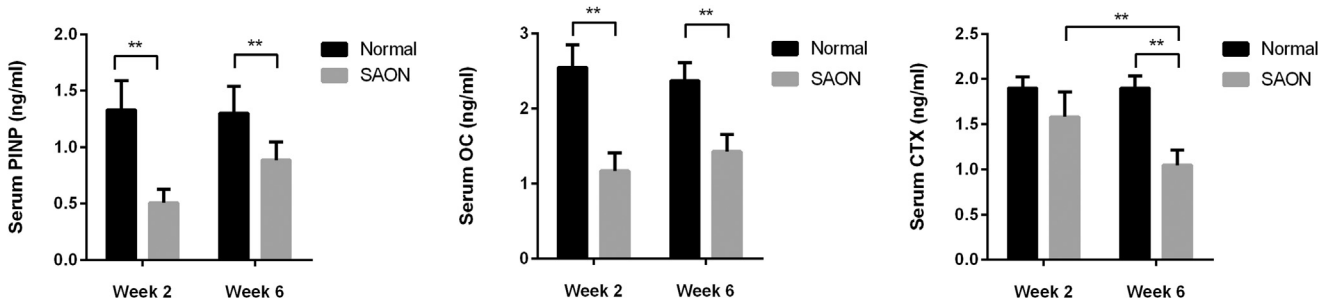

Figure 7 Serum markers. Bone turnover markers: serum PINP and OC in the SAON group were significantly lower at week 2 and week 6 than those in the normal group; serum CTX in the SAON group was significantly lower at week 6 than that in the normal group at the same time point and than that at week 2 in the SAON group. (*: $p < 0.05$, **: $p < 0.01$, n = 6).
CTX = carboxy-terminal telopeptide; OC = osteocalcin; PINP = amino-terminal propeptide of type I collagen; SAON = steroid-associated osteonecrosis.

hepatic cell, the adipocytes in the liver sections showed as oval cavity outside the hepatic cells (Fig. 8).

Discussion

The present study evaluated an SAON induction protocol in rats with combination injections of LPS and MPS with different evaluation approaches to examine the metabolic disorders on the bone and other affected cross-talking tissues. The endpoint evaluation is the ON incidence evaluated by histology, which is a gold standard to evaluate ON in an animal model [24]. We observed typical ON lesions in our histological slides for proximal and distal femur and proximal and distal tibia, with similar histopathological ON features seen in severe acute respiratory syndrome (SARS) patients who received large dose of corticosteroid with SAON developed at multiple skeletal sites, including hip, knee and ankle joint [26].

We found 100% ON incidence at week 2 attributed to combined effects of LPS and large dose of pulsed MPS treatment. Corticosteroid-induced ON was through its direct effects on bone cells to induce the apoptosis of osteoblasts and osteocytes so as to impair bone formation [27,28]. LPS-induced inflammation could inhibit bone formation and increase bone resorption, which simulated the inflammation deceases [29,30]. In this study, the Ob. S/BS was significantly lower at the time point of week 2, suggesting that the LPS and excess corticosteroid induced cell death with reduced osteoblast number. Correspondingly, the bone formation marker PINP was significantly lower, which suggested that the total bone formation function is inhibited and accompanied downregulation of another bone formation marker OC at week 2. OC is secreted by the osteoblast and is a marker of the activity of osteoblasts' activity of the entire skeleton within the body [31]; it is also a bone-regulated endocrine hormone to regulate energy metabolism [31]. The significantly decreased OC could induce abnormal glucose and adipose metabolism [32,33]. Our results showed that the bone marrow fat in the SAON group was significantly larger than that in the normal control group, which could decrease the blood supply in the bone marrow region. OC could also stimulate angiogenesis [34]. Corticosteroid has antiangiogenesis effect [35], which consequently impairs blood supply. Our Microfil and angiography results showed that the volume of blood vessels in red bone marrow region of the proximal tibia of the SAON group was significantly lower than that in the normal control group, evidence of impaired blood supply in bone marrow, and consequently the induced hypoxia would eventually cause osteonecrosis. Oedema was appeared at bone marrow at week 2 after SAON induction. It was reported that LPS-induced inflammation could induce vascular dysfunction and blood vessel leakage [36]. Our Microfil and angiography results also showed more leakage particles in the distal tibia 2 weeks after SAON induction. More leakage particles found in the present study suggested higher vessel permeability that could induce oedema, and

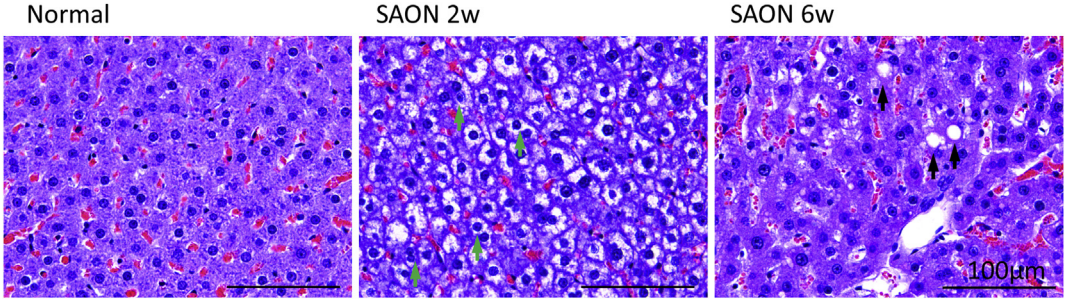

Figure 8 Liver histopathologic appearance. Representative H&E staining sections showed regular hepatic cells in normal rats, hepatic oedema and cell division (Green arrow) 2 weeks after SAON induction and fatty liver 6 weeks after SAON induction. (Black arrow: lipid accumulation).
SAON = steroid-associated osteonecrosis.

higher marrow pressure, in turn, reduced blood flow and induced hypoxia. The LPS-induced blood vessel leakage further induced oedema, then inhibited the blood vessel function and then hypoxia, which eventually induce osteonecrosis. VEGF expression was higher in the SAON group in both proximal and distal tibia, indicating severe ischaemia and hypoxia condition in the SAON group after induction.

Micro-CT—based trabecular architecture analysis demonstrated significant bone loss at trabecular bone of the proximal tibia 6 weeks after SAON induction, demonstrated by the significant lower BMD, BV/TV, Conn. D., Tb. N and significant higher Tb. Sp in the SAON group. Normally, the Tb. Th becomes thinner during bone loss, while in this ROI, the Tb. Th is relatively higher near the cortical bone and thinner in the middle region. Based on representative micro-CT 3-D images, we could find that the trabeculae in the middle region were almost disappeared in the SAON group; therefore, there was no significant thinner Tb. Th of the SAON group which remained relatively thicker trabeculae near the cortical bone. For the SMI in micro-CT analysis, 0 means ideal parallel plate structure, and 3 means ideal cylindrical rod structure, and the SMI between 0 and 3 is dependent on the volume ratio of rods and plates [37]. In this study, the inner more trabeculae with rod-like structure were almost lost, and the outer more trabeculae with plate-like structure degraded towards more rod-like structure in the SAON group, which explained no significant difference in the SMI between the two groups.

During development of ON, necrotic bone repair was accompanied by bone resorption of necrotic bone and reparative bone formation of new bone in this rat SAON model. At the beginning of the repair progress at week 2, bone histomorphometry evaluated in the proximal tibia showed significantly lower Ob. S/BS and higher osteoclast number in the SAON group, suggesting significant bone loss after induction. Bone resorption marker CTX in the SAON group and normal group were however not significantly different, whereas the bone formation marker PINP and OC in the SAON group were both significantly lower than those in the normal group, suggesting systemic bone loss under the influence of LPS and MPS induction. At week 6, because of the continuous steroid treatment and the continuous bone loss, both bone formation markers and bone resorption marker were lower for the SAON group than those in the normal group. Bone histomorphometry revealed that the Ob. S/BS correspondingly showed lower osteoblast number in the SAON group at week 6, which demonstrated the continuous inhibiting effect of the steroid. Severe fat accumulation was found in red marrow region, and more oedema persisted in yellow marrow region at week 6 than those at week 2 in SAON group, suggesting poor blood supply at week 6 when compared with that at week 2, although at week 6, there were only two rats in the SAON group classified as ON−, which was explained by on-going repairing progress and the significant bone loss especially in red marrow region of ROIs evaluated at proximal femur, distal femur and proximal tibia.

Besides bone tissue, we also used DXA to test the fat/lean composition in the SAON rat model for the first time for studying soft tissues around the SAON region. The ROI was chosen at the low limb because the fat percent in the normal control group was low, i.e., 1.5% from the result that provided reference data to study their alterations in the SAON group. There is muscle—bone crosstalk that they may modulate each other mechanically and metabolically [38], especially in the metabolic syndrome affected by excess corticosteroid [39]. Inflammation, oxidative stress and hormonal modification could be the common causes involved in development of decreased muscle mass and decreased osteoblast activity [38]. In our SAON rat model, we found significantly lower lean mass from DXA results and lower bone mass from micro-CT at week 6 that shared similar clinical features [39]. DXA results in this study also showed significantly increased fat percentage in the lower limb in the SAON group at week 6, whereas the body weight for rats from the SAON group did not increase from week 2 to week 6, suggesting that corticosteroid treatment changed the tissue composition, i.e., increased fat tissue and decreased bone and skeletal muscle, but not body weight in this rat SAON model. The excess corticosteroid treatment could affect differentiation potential of both adipocytes and osteoblasts by activating peroxisome proliferator-activated receptor gamma (PPARγ) of the precursor cells of adipocytes and osteoblasts to increase adipogenesis and meanwhile decrease osteogenesis to induce osteonecrosis [40,41].

The liver is a vital organ in metabolism, and disorders in the liver reflect the whole body pathophysiological metabolic disorders [42]. In this SAON rat model, the occurrence of hepatic oedema and cell division 2 weeks after SAON induction suggested the acute LPS-induced inflammation injury and liver cells repair progress, which were accompanied by development of osteonecrosis and its repair process at week 2. The fatty liver 6 weeks after SAON induction suggested abnormal high lipid levels in corticosteroid-affected metabolic disorders, which corresponded with the fat body including high fat levels in the body composition and high fat level in the bone marrow 6 weeks after SAON induction.

Compared with the previously published reports using combination of LPS and MPS with variant dosages and time window, the present study reported details on evaluations of osteonecrosis, together with additional important information on mortality rate, and other associated temporal changes in metabolism at two different time points that reflect the occurrences and repairing of osteonecrosis and steroid-associated bone loss.

In conclusion, the present study successfully induced SAON in a rat model with pulsed injection of LPS and MPS and evaluation protocols with typical histopathologic ON features and advanced evaluation approaches to identify the metabolic disorders of SAON. The SAON rat model is a suitable and cost-effective animal model to study cellular and molecular mechanism of SAON and potential drugs to be developed for prevention and treatment of SAON.

Conflicts of interest

All authors declare that they have no conflict of interest.

Acknowledgement

The work described on this article was fully supported by a grant from the Research Grants Council of the Hong Kong Special Administrative Region, China (Ref No. T13-402/17-N).

References

[1] Xie XH, Wang XL, Yang HL, Zhao DW, Qin L. Steroid-associated osteonecrosis: epidemiology, pathophysiology, animal model, prevention, and potential treatments (an overview). J Orthop Translat 2015;32:58—70.
[2] Weinstein RS. Clinical practice. Glucocorticoid-induced bone disease. N Engl J Med 2011;3651:62—70.
[3] Qin L, Zhang G, Sheng H, Yeung KW, Yeung HY, Chan CW, et al. Multiple bioimaging modalities in evaluation of an experimental osteonecrosis induced by a combination of lipopolysaccharide and methylprednisolone. Bone 2006;394:863—71.
[4] Bekler H, Uygur AM, Gökçe A, Beyzadeoğlu T. The effect of steroid use on the pathogenesis of avascular necrosis of the femoral head: an animal model. Acta Orthop Traumatol Turc 2007;411:58—63.
[5] Okazaki S, Nagoya S, Matsumoto H, Mizuo K, Shimizu J, Watanabe S, et al. TLR4 stimulation and corticosteroid interactively induce osteonecrosis of the femoral head in rat. J Orthop Res 2016;342:342—5.
[6] Okazaki S, Nishitani Y, Nagoya S, Kaya M, Yamashita T, Matsumoto H. Femoral head osteonecrosis can be caused by disruption of the systemic immune response via the toll-like receptor 4 signalling pathway. Rheumatology 2009;483: 227—32.
[7] Han N, Yan ZQ, Guo CA, Shen F, Liu J, Shi YX, et al. Effects of P-Glycoprotein on steroid-induced osteonecrosis of the femoral head. Calcif Tissue Int 2010;873:246—53.
[8] Ding S, Peng H, Fang HS, Zhou JL, Wang Z. Pulsed electromagnetic fields stimulation prevents steroid-induced osteonecrosis in rats. BMC Muscoskel Disord 2011:12.
[9] Okazaki S, Nishitani Y, Nagoya S, Kaya M, Yamashita T, Matsumoto H. Femoral head osteonecrosis can be caused by disruption of the systemic immune response via the toll-like receptor 4 signalling pathway. Rheumatology 2009;483: 227—32.
[10] Ben-Shaul V, Sofer Y, Bergman M, Zurovsky Y, Grossman S. Lipopolysaccharide-induced oxidative stress in the liver: comparison between rat and rabbit. Shock 1999;124:288—93.
[11] Zheng L, Wang X, Wang J, Qin L. Establishment of a cost-effective steroid associated osteonecrosis in rats. J Orthop Translat 2016;7(Suppl. C):116.
[12] Powell C, Chang C, Naguwa SM, Cheema G, Gershwin ME. Steroid induced osteonecrosis: an analysis of steroid dosing risk. Autoimmun Rev 2010;911:721—43.
[13] Nair AB, Jacob S. A simple practice guide for dose conversion between animals and human. J Basic Clin Pharm 2016;72:27—31.
[14] Quinn R. Comparing rat's to human's age: how old is my rat in people years? Nutrition 2005;216:775—7.
[15] Sun Y, Ma S, Zhou J, Yamoah AK, Feng JQ, Hinton RJ, et al. Distribution of small integrin-binding ligand, N-linked glycoproteins (SIBLING) in the articular cartilage of the rat femoral head. J Histochem Cytochem 2010;5811:1033—43.
[16] Resources IoLA. Guide for the care and used of laboratory animals. National Academies Press; 1996.
[17] Kilkenny C, Browne WJ, Cuthill IC, Emerson M, Altman DG. Improving bioscience research reporting: the ARRIVE guidelines for reporting animal research. PLoS Biol 2010;86: e1000412.
[18] Hou GQ, Guo C, Song GH, Fang N, Fan WJ, Chen XD, et al. Lipopolysaccharide (LPS) promotes osteoclast differentiation and activation by enhancing the MAPK pathway and COX-2 expression in RAW264.7 cells. Int J Mol Med 2013;322: 503—10.
[19] Bouxsein ML, Boyd SK, Christiansen BA, Guldberg RE, Jepsen KJ, Muller R. Guidelines for assessment of bone microstructure in rodents using micro-computed tomography. J Bone Miner Res 2010;257:1468—86.
[20] Zhang G, Qin L, Sheng H, Yeung KW, Yeung HY, Cheung WH, et al. Epimedium-derived phytoestrogen exert beneficial effect on preventing steroid-associated osteonecrosis in rabbits with inhibition of both thrombosis and lipid-deposition. Bone 2007;403:685—92.
[21] Duvall CL, Taylor WR, Weiss D, Guldberg RE. Quantitative microcomputed tomography analysis of collateral vessel development after ischemic injury. Am J Physiol Heart Circ Physiol 2004;2871:H302—10.
[22] Zhang G, Sheng H, He YX, Xie XH, Wang YX, Lee KM, et al. Continuous occurrence of both insufficient neovascularization and elevated vascular permeability in rabbit proximal femur during inadequate repair of steroid-associated osteonecrotic lesions. Arthritis Rheum 2009;6010:2966—77.
[23] Chen S-H, Wang X-L, Zheng L-Z, Dai Y, Zhang J-Y, Guo B-L, et al. Comparative study of two types of herbal capsules with different Epimedium species for the prevention of ovariectomised-induced osteoporosis in rats. J Orthop Translat 2016;4:14—27.
[24] Yamamoto T, Irisa T, Sugioka Y, Sueishi K. Effects of pulse methylprednisolone on bone and marrow tissues: corticosteroid-induced osteonecrosis in rabbits. Arthritis Rheum 1997;4011:2055—64.
[25] Dempster DW, Compston JE, Drezner MK, Glorieux FH, Kanis JA, Malluche H, et al. Standardized nomenclature, symbols, and units for bone histomorphometry: a 2012 update of the report of the ASBMR histomorphometry nomenclature committee. J Bone Miner Res 2013;281:2—17.
[26] Sun W, Shi Z, Gao F, Wang B, Li Z. The pathogenesis of multifocal osteonecrosis. Sci Rep 2016;6:29576.
[27] Weinstein RS. Glucocorticoid-induced osteoporosis and osteonecrosis. Endocrinol Metab Clin North Am 2012;413: 595—611.
[28] O'Brien CA, Jia D, Plotkin LI, Bellido T, Powers CC, Stewart SA, et al. Glucocorticoids act directly on osteoblasts and osteocytes to induce their apoptosis and reduce bone formation and strength. Endocrinology 2004;1454:1835—41.
[29] Feng X, McDonald JM. Disorders of bone remodeling. Annu Rev Pathol: Mech Dis 2011;6(6):121—45.
[30] Hardy R, Cooper MS. Bone loss in inflammatory disorders. J Endocrinol 2009;2013:309—20.
[31] Lee NK, Sowa H, Hinoi E, Ferron M, Ahn JD, Confavreux C, et al. Endocrine regulation of energy metabolism by the skeleton. Cell 2007;1303:456—69.
[32] Kanazawa I. Osteocalcin as a hormone regulating glucose metabolism. World J Diabetes 2015;618:1345—54.
[33] Foresta C, Strapazzon G, De Toni L, Gianesello L, Calcagno A, Pilon C, et al. Evidence for osteocalcin production by adipose tissue and its role in human metabolism. J Clin Endocrinol Metabol 2010;957:3502—6.
[34] Cantatore FP, Crivellato E, Nico B, Ribatti D. Osteocalcin is angiogenic in vivo. Cell Biol Int 2005;297:583—5.
[35] Folkman J, Ingber DE. Angiostatic steroids - method of discovery and mechanism of action. Ann Surg 1987;2063: 374—83.
[36] Niessen F, Furlan-Freguia C, Fernandez JA, Mosnier LO, Castellino FJ, Weiler H, et al. Endogenous EPCR/aPC-PAR1 signaling prevents inflammation-induced vascular leakage

and lethality (Retracted article. See vol. 117, pg. 7188, 2011). Blood 2009;11312:2859—66.
[37] Hildebrand T, Ruegsegger P. Quantification of bone microarchitecture with the structure model index. Comput Meth Biomech Biomed Eng 1997;11:15—23.
[38] Tagliaferri C, Wittrant Y, Davicco MJ, Walrand S, Coxam V. Muscle and bone, two interconnected tissues. Ageing Res Rev 2015;21:55—70.
[39] Schacke H, Docke WD, Asadullah K. Mechanisms involved in the side effects of glucocorticoids. Pharmacol Ther 2002;961:23—43.
[40] Zhang G, Qin L, Sheng H, Wang XL, Wang YX, Yeung DK, et al. A novel semisynthesized small molecule icaritin reduces incidence of steroid-associated osteonecrosis with inhibition of both thrombosis and lipid-deposition in a dose-dependent manner. Bone 2009;442:345—56.
[41] Cui Q, Wang GJ, Su CC, Balian G. The Otto Aufranc Award. Lovastatin prevents steroid induced adipogenesis and osteonecrosis. Clin Orthop Relat Res 1997;344:8—19.
[42] Hotamisligil GS. Inflammation and metabolic disorders. Nature 2006;444(7121):860—7.